

## Supporting Information

### Experimental and theoretical evidence of ion engineering in nanocrystalline molybdenum disulfide memristor for non-filamentary switching actions and ultra-low-voltage synaptic features

D. Das<sup>†\*</sup>, J. Asirvatham<sup>†</sup>, MA. Luong<sup>#</sup>, A. Claverie<sup>#</sup>, P. Johari<sup>†\*</sup> and A. Kanjilal<sup>†\*</sup>

<sup>†</sup>Department of Physics, School of Natural Sciences, Shiv Nadar University, NH-91, Dadri, Gautam Buddha Nagar, Uttar Pradesh 201314, India

<sup>#</sup> CEMES-CNRS, 29 Rue Jeanne Marvig, 31055 Toulouse, France

\*Corresponding authors: [dd209@snu.edu.in](mailto:dd209@snu.edu.in), [priya.johari@snu.edu.in](mailto:priya.johari@snu.edu.in),  
[aloke.kanjilal@snu.edu.in](mailto:aloke.kanjilal@snu.edu.in)

**Keywords:** Nanoengineering, 2D materials, Non-filamentary memristors, Neuromorphic electronics, DFT, Artificial neural network

## **Table of Contents**

1. Thickness and roughness measurements
2. Asymmetry analysis
3. Endurance of sample  $S_1$
4. Endurance of sample  $S_3$
5. Bending test
6. Alteration of layer thickness, current, and conductance variations with the applied voltage
7. SEM results
8. Band structure calculations
9. vdW corrections
10. Top and side view of the Na-diffusion path

## 1. Thickness and roughness measurements

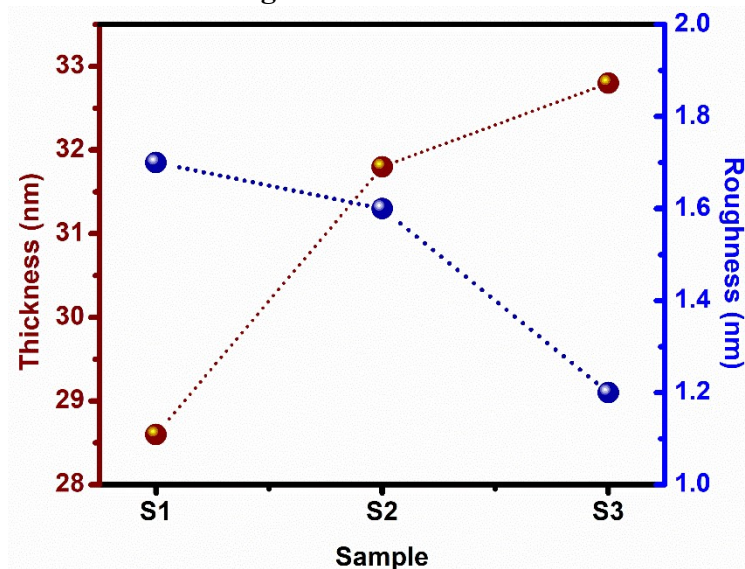


**Figure S1.** The thickness (roughness) of samples S<sub>1</sub>, S<sub>2</sub>, and S<sub>3</sub> was 28.6 (1.7), 31.8 (1.6), and 32.8 (1.2), respectively, measured using Bruker DektakXT surface profilometer.

## 2. Asymmetry analysis

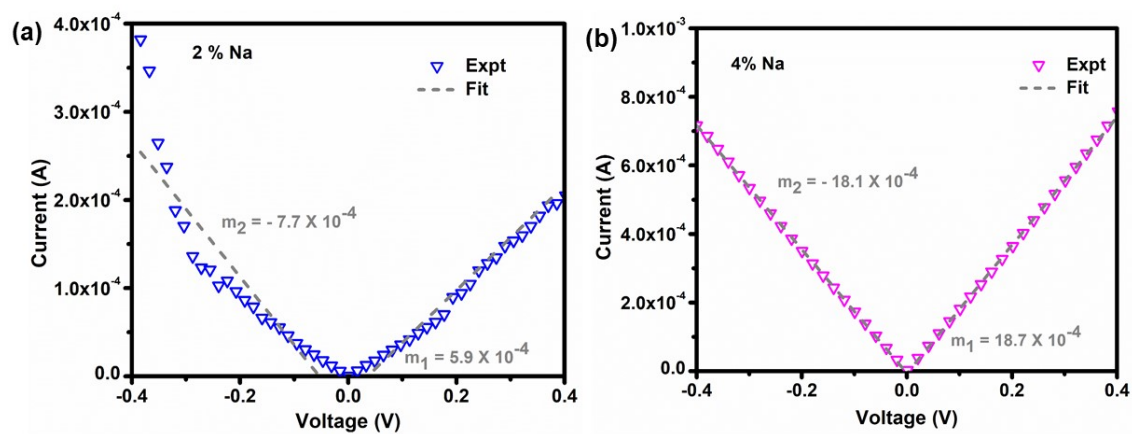


**Figure S2:** Current-voltage curves of (a) 2 wt. % Na and (b) 4 wt. % of Na fitted with a linear equation. It reveals the asymmetric nature of 2 wt. % Na.

### 3. Endurance of sample $S_1$

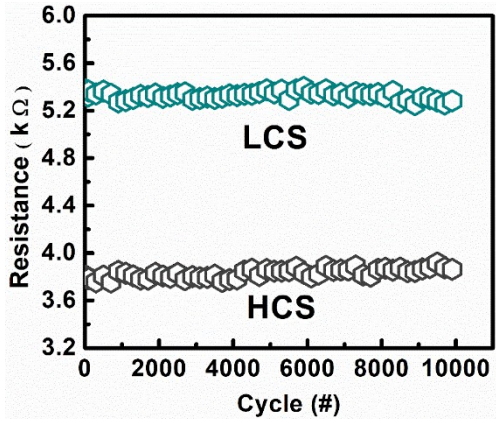


Figure S3. Endurance characteristics of sample  $S_1$  for up to  $10^3$  cycle

### 4. Endurance of sample $S_3$

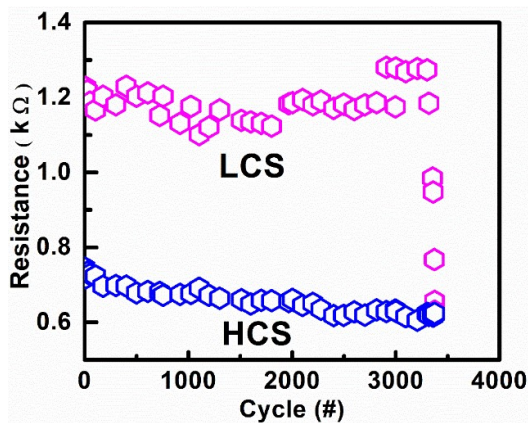


Figure S4. Endurance characteristics of sample  $S_3$ , after 3400 cycles the LCS merged to HCS.

### 5. Bending test

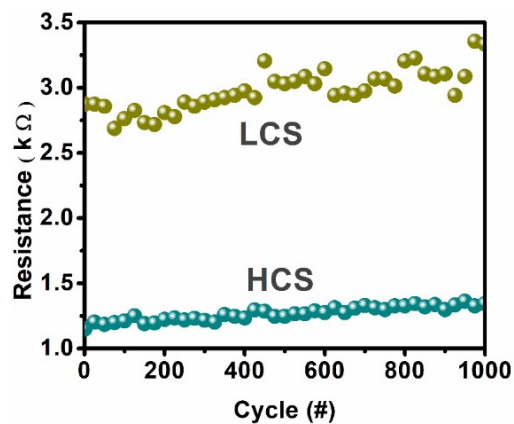


Figure S5. Device response with bending cycle

6. Alteration of layer thickness, current, and conductance variations with the applied voltage

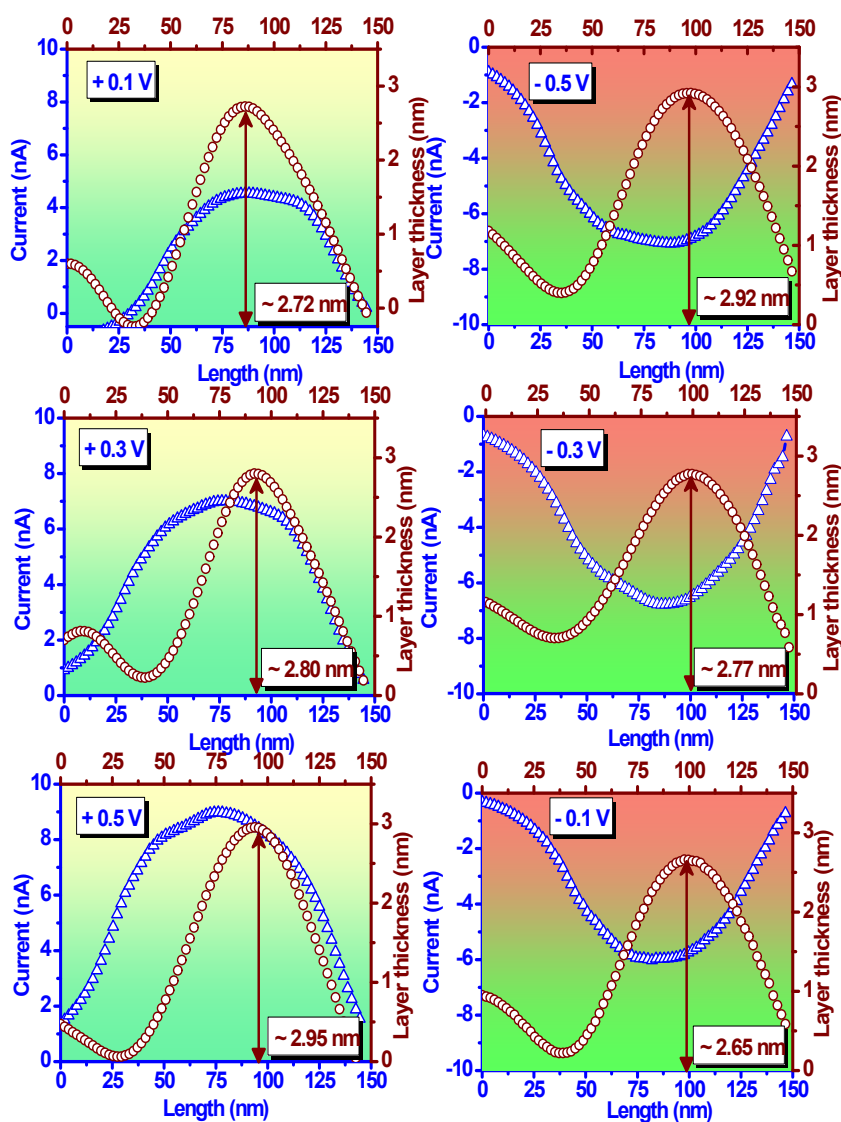
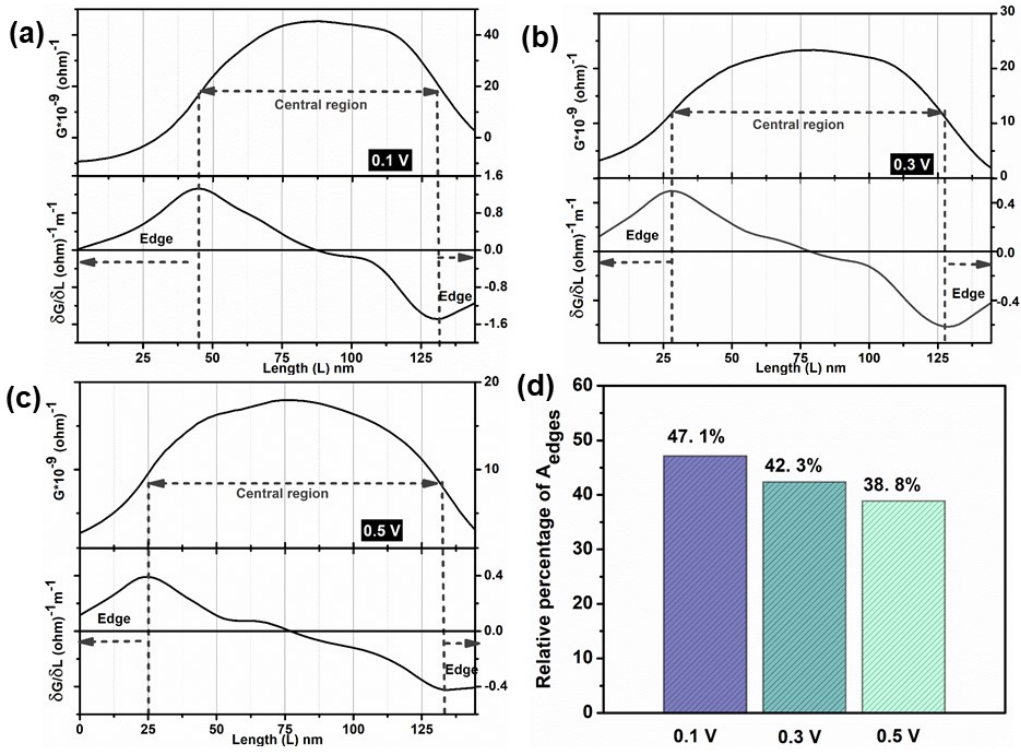


Figure S6. Change of layer thickness and current with applied bias.



**Figure S7:** Conductance variations (top) and its first-order space derivative (bottom panel) at the edges and the central region of the nanocrystal for three different applied voltages (a) 0.1V, (b) 0.3V and (c) 0.5 V; (d) Presents the relative area percentage of  $A_{edges}$  with  $A_{centre}$  for 0.1V, 0.3V, and 0.5V

We derive the conductance ( $G$ ) distribution along the nanocrystal's surface from the current scan. It is shown at the top panels of Figure S7 a-c. Subsequently, we calculate its first-order space derivative (i.e.,  $\delta G / \delta L$ , at the bottom panels of Figure S7 a-c), which relates to the carrier density [Reports on Progress in Physics 83.3 (2020): 036501]. Then, we calculate the area under the curve for two different regions, which are marked as edge and central regions in Figure S6 a-c.

$$A = A_{edges} + A_{centre} = \int_{edges} \left( \frac{\delta G}{\delta L} \right) dL + \int_{centre} \left( \frac{\delta G}{\delta L} \right) dL$$

Finally, we determine the relative percentage change of  $A_{edges}$  with  $A_{centre}$  for the three different potentials of 0.1V, 0.3V, and 0.5V (as shown in Figure S7d). It shows that the initial  $A_{edges}$  percentage was 47.1% for 0.1V and then drops to 38.8% for 0.5V. Therefore, it is reasonable to claim that the edges of nanocrystals become less conducting as the electric potential increases. Furthermore, a relative decrease in  $A_{edges}$  implies an increase in  $A_{centre}$ , and an increase in  $A_{centre}$  suggests an increase in carrier density (present case Na-ion) at the central region. As a result, we may reasonably argue that as potential increases, more Na-ions move from the edges to the central region.

## 7. Scanning electron microscopy results

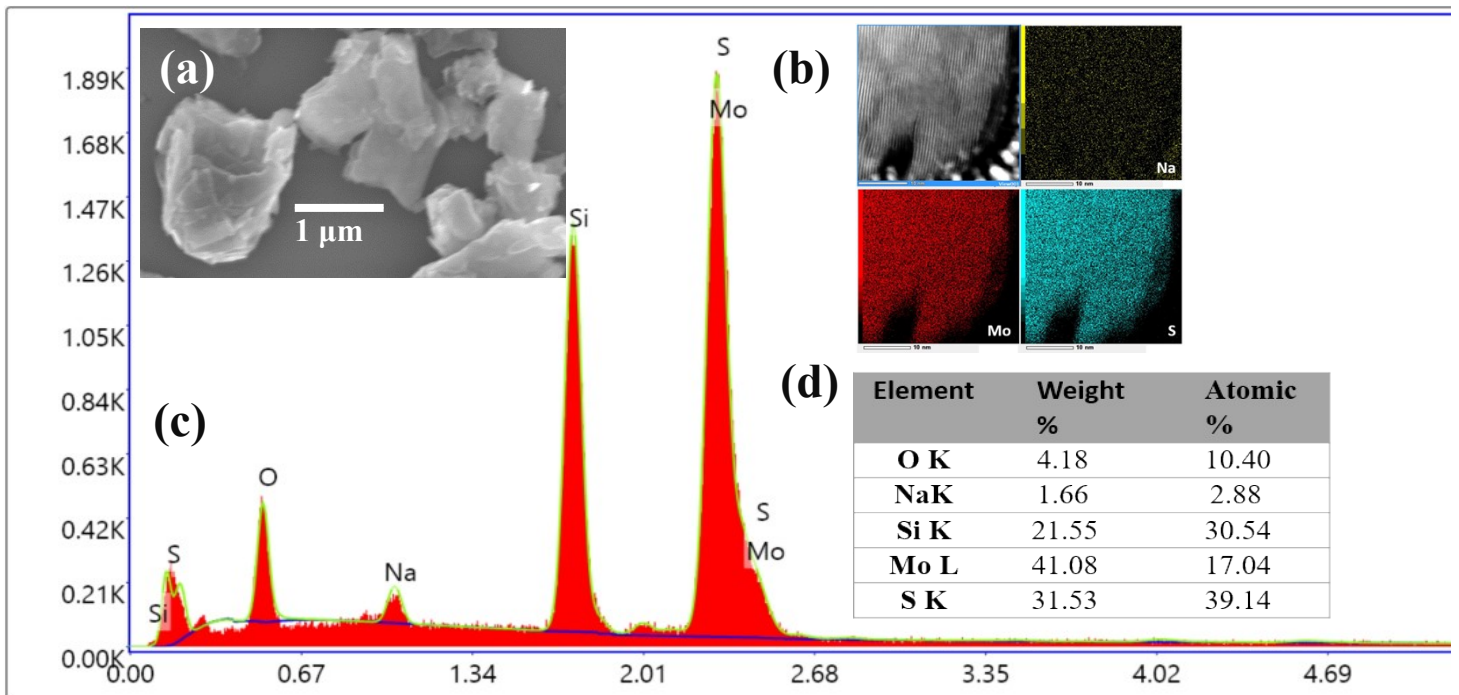


**Figure S8** (a) High-resolution SEM image of Na:MoS<sub>2</sub> flakes (b) Elemental analysis of the fabricated Na:MoS<sub>2</sub> flakes using energy-dispersive X-ray spectroscopy (EDX) technique. The distribution maps of Na, Mo, and S are presented in yellow, red, and cyan colors, respectively (c) Spectral distribution, and (d) atomic concentration.

## 8. Band structure and PDOS

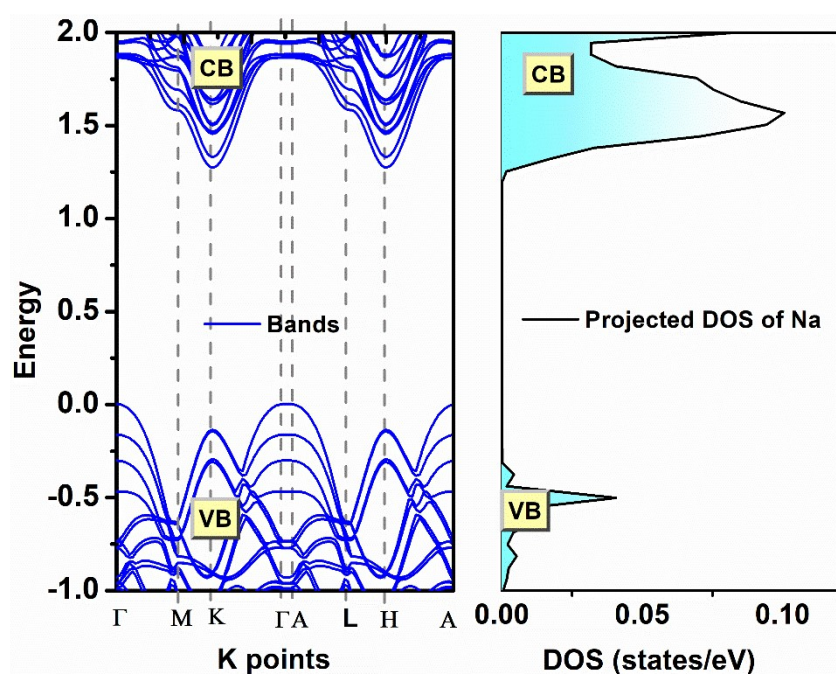


**Figure S9:** Band structure calculations along with the Na-projected density of states to show the influence of Na at the bottom of the conduction band.

## 9. vdW correction (DFT-D3 method)

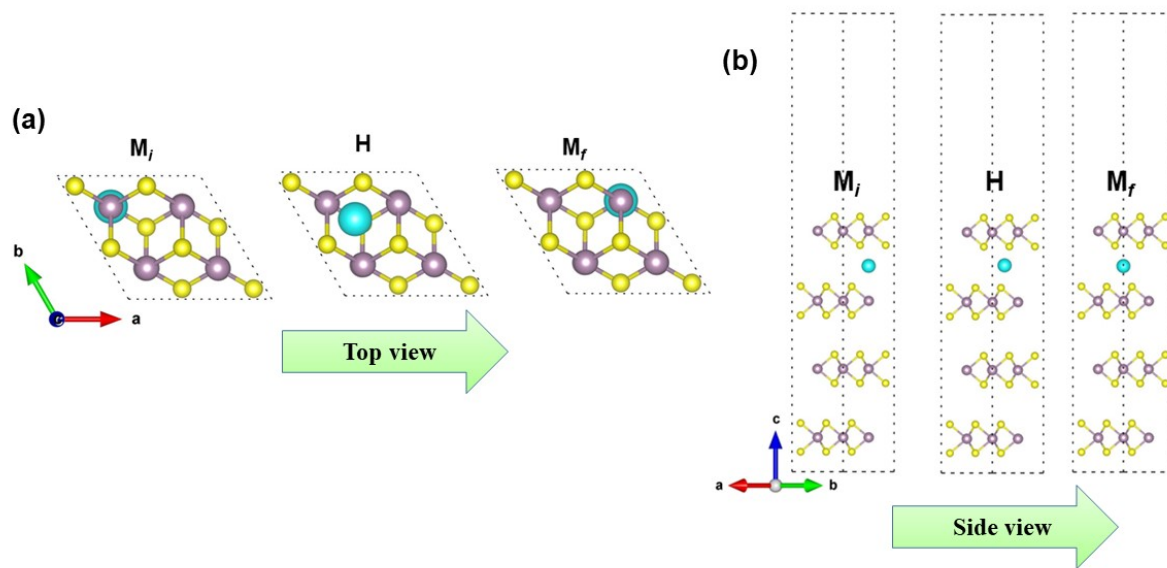
**Table S1:** Total energy of pristine and Na:MoS<sub>2</sub> using PBE and vdW (D3) method

	vdW correction	
	Without vdW correction (PBE)	With dipole



		<b>dipole correction</b>	<b>correction</b>
Pristine $E_{MoS_2}$	-348.772	-366.936	-366.935
Na: MoS <sub>2</sub> ( $E_{Na + MoS_2}$ )	-350.773	-368.938	-368.938
Difference in energy ( $E_{Na + MoS_2} - E_M$ )	-2.001	-2.002	2.003

*We checked the impact of vdW correction in our simulations using the DFT-D3 method with Becke-Johnson damping [Journal of computational chemistry 32.7 (2011): 1456-1465] to show the invariance of our results against different DFT functional. The details of the simulations are listed below. An overall shift in ground state energy at the lower energy side was noticed for the vdW correction (as compared with the standard PBE functional) in both the pristine MoS<sub>2</sub> and Na: MoS<sub>2</sub> systems. However, their relative change in energy is remaining unaltered; it proposes that our general arguments remain intact for other functionals.*



## 10. Na-diffusion path

**Figure S10.** The Na diffusion path (a) top view (b) side view.